Marquette University
e-Publications@Marquette

Chemistry Faculty Research and Publications

Chemistry, Department of

2-1-2004

Poly(Methyl Methacrylate), Polypropylene and Polyethylene Nanocomposite Formation by Melt Blending using Novel Polymerically-Modified Clays

Shengpei Su
Marquette University

David D. Jiang
Marquette University

Charles A. Wilkie
Marquette University, charles.wilkie@marquette.edu

Chemistry Faculty Research and Publications/College of Arts and Sciences

Poly(methyl methacrylate), Polypropylene and Polyethylene Nanocomposite Formation by Melt Blending Using Novel Polymerically-modified Clays

Shengpei Su
Department of Chemistry, Marquette University, Milwaukee, WI
David D. Jiang
Department of Chemistry, Marquette University, Milwaukee, WI
Charles A. Wilkie
Department of Chemistry, Marquette University, Milwaukee, WI

Abstract

Two new organically-modified clays that contain an oligomeric styrene or methacrylate have been prepared and used to produce nanocomposites of poly(methyl methacryate), polypropylene and polyethylene. Intercalated nanocomposites and, in some cases, exfoliated or mixed intercalated/exfoliated nanocomposites of all of these polymers have been produced by melt blending in a Brabender mixer. The use of the styrene-containing clay

permits the direct blending of the clay with polypropylene, without the usual need for maleation, to produce the nanocomposites. The systems have all been characterized by X-ray diffraction, transmission electron microscopy, thermogravimetric analysis, cone calorimetry and the measurement of mechanical properties. These novel new clays open new opportunities for melt blending of polymers with clays to obtain nanocomposites with important properties.

Keywords

Nanocomposites, Poly(methyl methacrylate), Polyolefins, Fire retardancy

1. Introduction

It is now well-known that one can enhance the properties of a polymer through the formation of a nanocomposite of that material. It is generally believed that nanocomposite formation may enhance the heat distortion temperature, permeability, fire retardancy and flexural modulus of polymers. In some instances the type of nanocomposite, intercalated or exfoliated, is very important while in others, notably fire retardancy, both intercalated and exfoliated systems show the same behavior.

The preparation of nanocomposites has been accomplished both by polymerization and by blending. For many materials, the polymerization process is not available or convenient and a blending process is preferred. Since the thermal degradation of many organically-modified clays begins at temperatures as low as 200 °C, clays with enhanced thermal stability are desired. An additional requirement is that the organically-modified clay have good compatibility with the polymer with which it is to be blended.

In the accompanying paper we describe the preparation of two new organically-modified clays that may be used to produce nanocomposite by melt blending [1]. In this paper we extend these results by preparing and fully characterizing nanocomposites of poly(methyl methacrylate), polypropylene and polyethylene.

2. Experimental

2.1. Materials

The majority of chemicals used in this study, including vinylbenzyl chloride, styrene, benzoyl peroxide (BPO), *N*,*N*-dimethylhexadecylamine, inhibitor removal reagents, PMMA [crystals, *Mw*=996,000 (GPC), inherent viscosity 1.25], PE (melt flow index, 190 °C/2.16 kg, 7 g/10 min), PP (isotactic, melt flow index, 230 °C/2.16 kg, 35 g/10 min) were acquired from Aldrich Chemical Co. Pristine sodium montmorillonite was provided by Southern Clay Products, Inc.

2.2. Instrumentation

Thermogravimetric analysis (TGA) was performed on a Cahn TG-131 instrument under a flowing nitrogen atmosphere at a scan rate of 10 °C/min from 20 to 600 °C. All TGA results are the average of a minimum of three determinations; temperatures are reproducible to ±3 °C, while the error bars on the fraction of nonvolatile material is ±3%. Cone calorimetry was performed using an Atlas Cone 2 instrument according ASTM E 1354-92 at an incident flux of 35 or 50 kW/m^2 using a cone shaped heater. Exhaust flow was set at 24 l/s and the spark was continuous until the sample ignited. Cone samples were prepared by compression molding the sample (20–50 g) into square plaques using a heated press. Typical results from Cone calorimetry are reproducible to within about ±10%. These uncertainties are based on many runs in which thousands of samples have been combusted [2], [3]. X-ray diffraction was performed on a Rigaku Geiger Flex, 2-circle powder diffractometer; scans were take from 2 theta 0.86–10, step size 0.1, and scan time per step of 10 s. Bright field transmission electron microscopy (TEM) images of the composites were obtained at 60 kV with a Zeiss 10 c electron microscope or a Jeol 100CX electron microscope equipped with an AMT digital system. The samples were ultramicrotomed with a diamond knife on

Riechert-Jung Ultra-Cut E microtome at room temperature or cryogenic temperatures or on a Sorvall MT-2B microtome at room temperature to give ~70 nm thick sections. PP and PE nanocomposites were cut using cryogenic conditions. The sections were transferred from the knife-edge to 600 hexagonal mesh Cu grids. The contrast between the layered silicates and the polymer phase was sufficient for imaging, so no heavy metal staining of sections prior to imaging is required. Some images were obtained using digital technology; the highest magnification cannot be achieved with this system since the resolution of the camera is limited. Mechanical properties were obtained using a SINTECH 10 (Systems Integration Technology, Inc.) computerized system for material testing at a crosshead speed of 0.2 in/min. The samples were prepared both by injection molding, using an Atlas model CS 183MMX mini max molder, and by stamping from a sheet; the reported values are the average of five determinations.

2.3. Molecular weight determination

The molecular weight of the copolymer was determined by viscosity measurements. The Mark-Houwink constants [4] of PS or PMMA were used, since the copolymer was 95% PS or 95% PMMA.

The synthesis of the copolymers, their ammonium salts and the clays have all been described in the accompanying paper.

2.4. Preparation of polymer–clay nanocomposites

All the nanocomposites were prepared by melt blending in a Brabender Plasticorder at high speed (60 rpm) at 200 °C for PMMA and 190 °C for PP and PE. The composition of each nanocomposite is calculated from the amount of clay and polymer charged to the Brabender.

3. Results and discussion

It is known that the process that is to be used for nanocomposite formation determines the characteristics of the organic modification that is required for the clay. For instance one long alkyl chain is required to prepare a styrene nanocomposite by a polymerization process, while two chains are required for melt blending [2], [5]. In addition, to prepare nanocomposites of polypropylene, it is normally necessary to begin with maleated polypropylene, PP-g-MA, and to combine this with polypropylene [6]. A goal of this work was to evaluate two new clays, both of which contain oligomeric fractions, one a styrene oligomer and the other a methacrylate oligomer, with poly(methyl methacrylate), PMMA, polypropylene, PP, and polyethylene, PE. Of particular interest was the preparation of PP nanocomposites without the need for PP-g-MA.

The copolymers that have been prepared have molecular weights in the range of 5000–6000 and contain about 5 mass% vinylbenzyl chloride, which corresponds to 1–2 ammonium salts per unit. The reader will notice that the fraction of organically-modified clay is much larger than is normally used. Because the molecular weight of the ammonium salt is near 5000 (meaning that the salt is about 29% aluminosilicate), while the normal ammonium salt has a molecular weight near 400 (78% aluminosilicate), one must add much more in order to maintain the fraction of aluminosilicate. Thus at 25% loading of the organically-modified clay, there is 7% aluminosilicate present while at 15% loading, there is 4% alumniosilicate present.

3.1. XRD measurement

The d-spacing of the sodium clay is 1.2 nm and this increases to 8.1 nm when the ammonium salt of COPS replaces the sodium cation. The XRD traces for the clays and their nanocomposites with PMMA, PP and PE are shown in Fig. 1, Fig. 2, Fig. 3, Fig. 4, Fig. 5, Fig. 6, respectively. For PMMA and PE, no peaks can be seen in the XRD of the COPS material and this suggests that these are either exfoliated systems or that a significant amount of disorder has occurred. A weak peak can be observed with COPS-PP, suggesting intercalation. For MAPS, peaks are clearly seen for PMMA, possibly for PP and no peak is observed for PE.
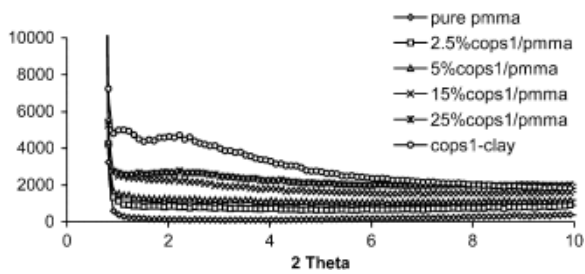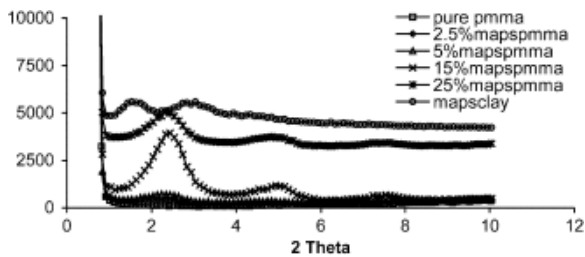
Fig. 1. XRD for COPS-PMMA nanocomposites.
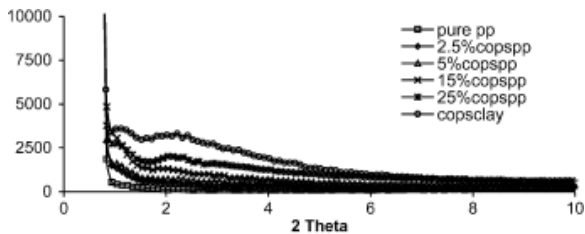

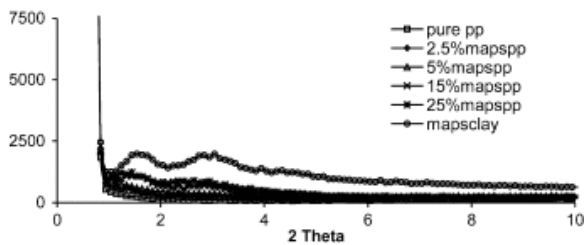Fig. 2. XRD for MAPS-PMMA nanocomposites.

Fig. 3. XRD for COPS-PP nanocomposites.

Fig. 4. XRD for MAPS-PP nanocomposites.
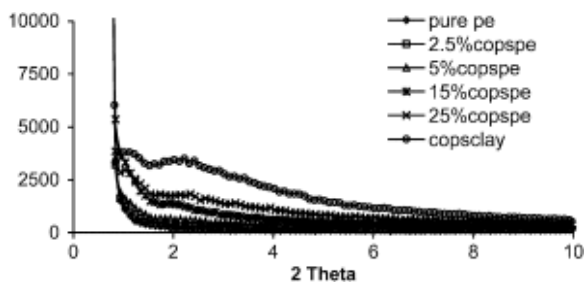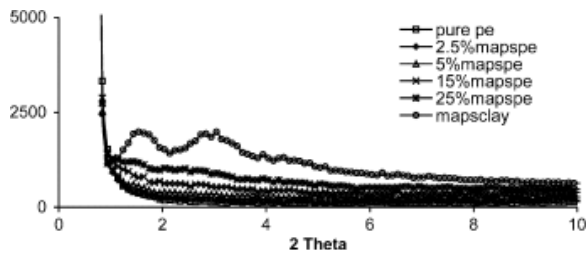

Fig. 5. XRD for COPS-PE nanocomposites.

Fig. 6. XRD for MAPS-PE nanocomposites.

The summation of the XRD results is that when peaks are seen in the XRD, they are generally broader for MAPS than for COPS, which may indicate a tendency to disordering for MAPS. The XRD data provides the first piece of information to indicate the type of nanocomposite that has been formed and TEM is now required to complete the description.

3.2. TEM results

The TEM images at both low and high magnification for both the organically-modified clays and the nanocomposites with PMMA, PP and PE are shown in Fig. 7, Fig. 8, Fig. 9, Fig. 10, Fig. 11, Fig. 12, Fig. 13. It must be noted that some images were obtained using digital technology and this does not permit as high a magnification as is possible using film. Images that were obtained using the digital technology are shown with scale bars at 2 μm and at 100 nm while those obtained using film are shown with scale bars of 200 and 50 nm. The images for both COPS and MAPS clays are shown in the accompanying paper and it is clear that good nanodispersion is seen for COPS while tactoids are present for MAPS.

Fig. 7. TEM image at low (left) and high (right) magnification of the COPS-PMMA nanocomposite.

Fig. 8. TEM image at low (left) and high (right) magnification of the MAPS-PMMA nanocomposite.

Fig. 9. TEM image at low (left) and high (right) magnification of the solution blended MAPS-PMMA nanocomposite.

Fig. 10. TEM image at low (left) and high (right) magnification of the COPS-PP nanocomposite.

Fig. 11. TEM image at low (left) and high (right) magnification of the MAPS-PP nanocomposite.
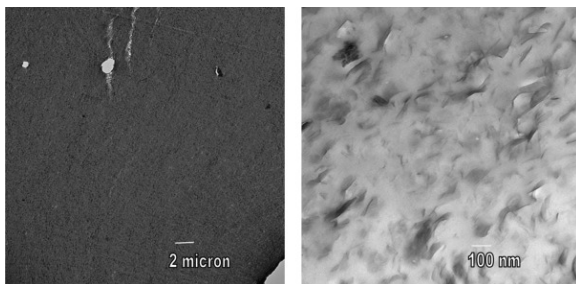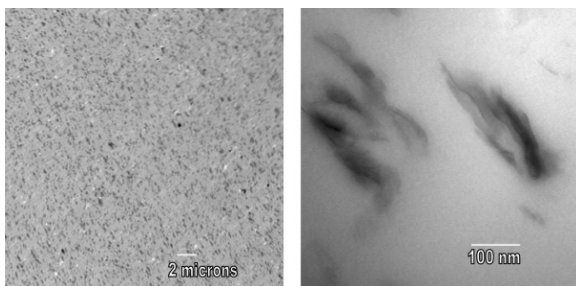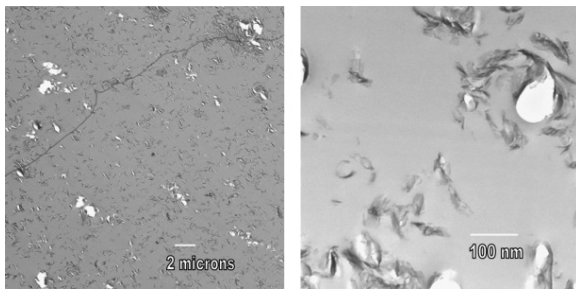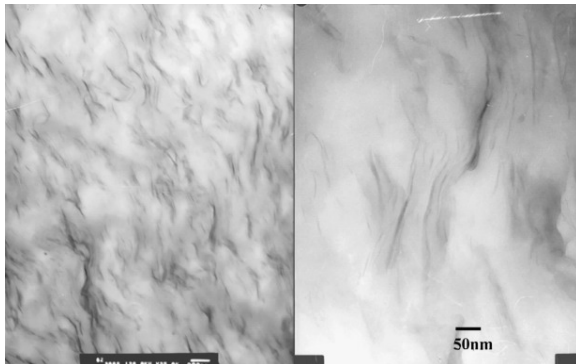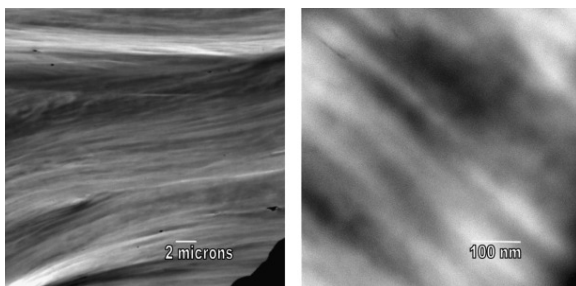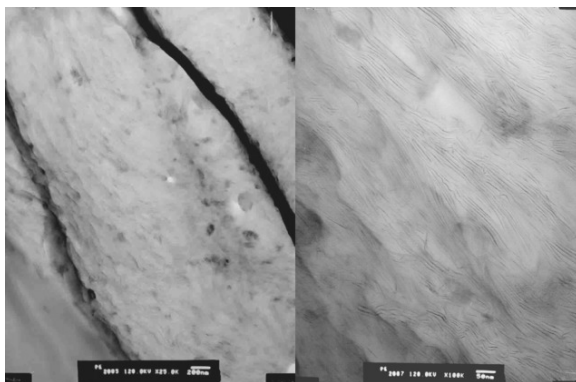

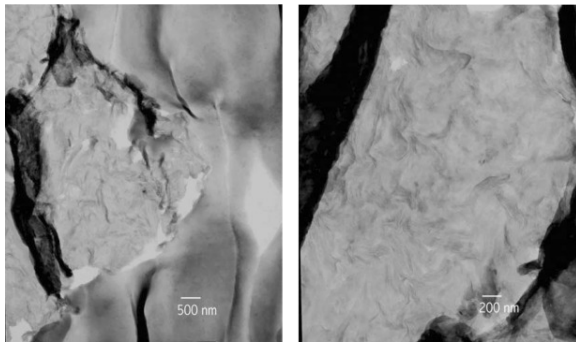Fig. 12. TEM image at low (left) and high (right) magnification of the COPS-PE nanocomposite.

Fig. 13. TEM image at low (left) and high (right) magnification of the MAPS-PE nanocomposite.

The two clays behave similarly for PMMA, Fig. 7, Fig. 8. At low magnification, one can see that there is nanodispersion of the clay within the polymer. At higher magnification, tactoids, and no individual clay layers, are seen for MAPS while for COPS primarily individual clay layers may be observed. The absence of an XRD peak in COPS-PMMA suggests exfoliation, which may also be inferred from the TEM. Solution blending also had been used for the MAPS-PMMA system (Fig. 9). Nanodispersion is quite good but tactoids, rather than individual clay layers, are seen at high magnification.

The images of PP and PE are shown in Fig. 10, Fig. 11, Fig. 12, Fig. 13. In all cases, the low magnification images show that nanodispersion has been achieved. In the case of COPS, one can see individual clay layers, which should be described as intercalated for PP and, perhaps, a mixture of intercalated and exfoliated for PE. It is quite possible that under conditions of greater shear, as may be obtained with a twin screw extruder, one may be able to directly obtain an exfoliated polypropylene nanocomposite. It must be noted that previous workers have made polypropylene nanocomposites using maleated polypropylene, i.e., PP-g-MA, and, in some cases, intercalated systems have been produced.

It is clear from these results that COPS is more likely to show individual clay layers while clay tactoids are frequently observed with MAPS. It is surprising that MAPS-PMMA is immiscible and not intercalated or exfoliated since one might expect the compatibility between the clay and polymer to be very high. The observation that COPS gives intercalated or exfoliated nanocomposites with PP and PE may be expected from the non-polar nature of styrene and the polyolefins. Likewise the immiscible character of MAPS-PP and MAPS-PE can probably be explained through differences in polarity.

3.3. TGA characterization of the nanocomposites

The thermal stability of the nanocomposites has been accessed using TGA; the parameters are shown in Table 1 for COPS-polymer systems and in Table 2 for MAPS-polymer systems and include the temperature at which 10% degradation occurs, a measure of the onset of degradation, the temperature at which 50% degradation occurs, the mid-point of the degradation process, and the fraction of material which remains at 600 °C, denoted as char [7]. These results are also presented graphically for each of the polymer systems studied in Fig. 14, Fig. 15, Fig. 16, Fig. 17, Fig. 18, Fig. 19. It is clear from there data that the COPS clay has enhanced thermal stability relative to the MAPS clay. This is not surprising, since PS has a higher thermal stability than does PMMA. For COPS-PMMA, the nanocomposite and the virgin polymer show about the same temperatures for any degree of degradation while for MAPS-PMMA the onset temperature of the degradation is higher for the nanocomposite than for the polymer and it increases as the amount of clay increases. Previous work on PMMA nanocomposites has shown that the nanocomposite is usually slightly more thermally stable than the virgin polymer [8].

Table 1. TGA data for COPS Ananocomposites

Material	T_{10} (°C)	T_{50} (°C)	Char (%)
Pure PMMA	275	340	2
2.5%COPS/PMMA	280	345	2
5% COPS/PMMA	287	357	2
15% COPS/PMMA	287	352	6
25% COPS/PMMA	285	363	8
Pure PP	319	406	0
2.5%COPS/PP	324	413	2
5% COPS/PP	330	414	2
15% COPS/PP	333	408	4
25% COPS/PP	340	414	8
Pure PE	390	464	2
2.5%COPS/PE	394	465	3
5%COPS/PE	396	465	3
15%COPS/PE	398	466	4
25%COPS/PE	398	466	8

Table 2. TGA data for MAPS Ananocomposites

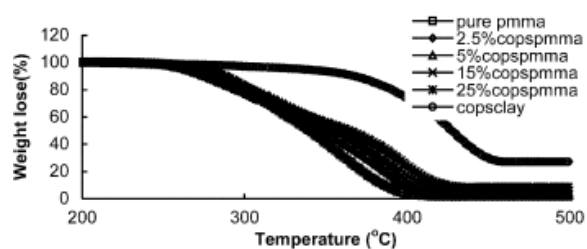| Material	T_{10} (°C)	T_{50} (°C)	Char (%)
Pure PMMA	275	340	2
2.5%MAPS/PMMA	291	347	1
5% MAPS/PMMA	303	359	4
15% MAPS/PMMA	297	362	7
25% MAPS/PMMA	301	376	9
Pure PP	319	406	0
2.5%MAPS/PP	333	424	2
5%MAPS/PP	323	423	3
15%MAPS/PP	315	416	6
25%MAPS/PP	311	409	7
Pure PE	390	464	2
2.5%MAPS/PE	403	473	2
5%MAPS/PE	396	476	2
15%MAPS/PE	378	471	5
25%MAPS/PE	367	465	8

Fig. 14. TGA curves for COPS-PMMA nanocomposites.
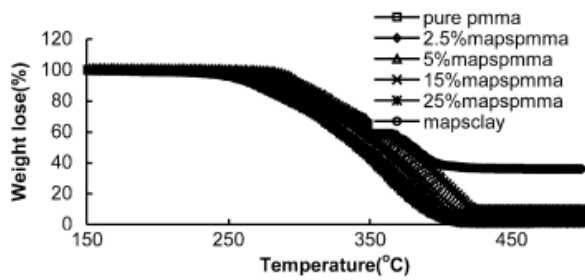
Fig. 15. TGA curves for MAPS-PMMA nanocomposites.
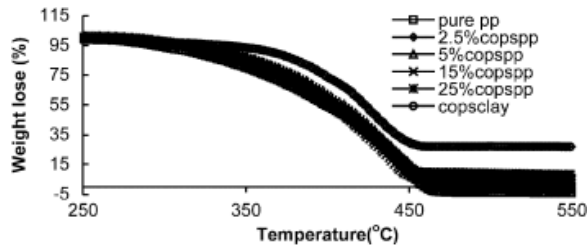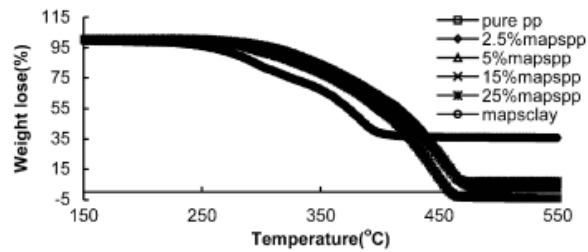

Fig. 16. TGA curves for COPS-PP nanocomposites.

Fig. 17. TGA curves for MAPS-PP nanocomposites.

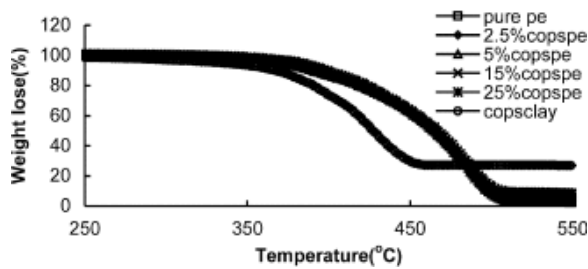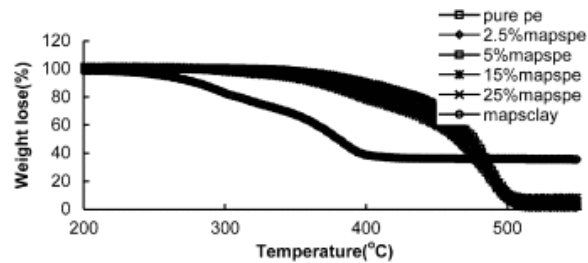Fig. 18. TGA curves for COPS-PE nanocomposites.

Fig. 19. TGA curves for MAPS-PE nanocomposites.

For PP and PE nanocomposites prepared with either clay, there is little difference in the temperatures for any clay level and for the virgin polymer, i.e., nanocomposite formation has no effect on the thermal stability of the polymer. PE nanocomposites are more thermally stable than either COPS or MAPS clays while MAPS-PP nanocomposites are more thermally stable and COPS-PP nanocomposites are less thermally stable than the clays. In previous work from these laboratories it has been shown that the thermal stability of PE and its nanocomposites, as measured by TGA, are the same [9]. It is known that polyethylene is more thermally stable than is polypropylene, presumably due to the presence of tertiary carbons in PP and their absence in PE, making for easier bond cleavage in PP than in PE [10].

3.4. Cone calorimetric characterization of the nanocomposites

The various parameters that may be evaluated using cone calorimetry, including the time to ignition, t_{ign}, the peak heat release rate, PHRR and the time to PHRR, t_{PHRR}, the mass loss rate, MLR, and the specific extinction area, SEA, a measure of the amount of smoke evolved, are tabulated in Table 3, Table 4 for PMMA. There is a significant difference between COPS and MAPS. In both cases the total heat released is constant and the maximum reduction in PHRR is much smaller than seen for PS. This has been previously seen when comparing PS and PMMA nanocomposites. There is a smaller reduction in PHRR and a greater increase in smoke for COPS-PMMA and the time to ignition increases as the amount of clay increases. For MAPS, the time to ignition is constant and the increase in smoke is much smaller, while the decrease in mass loss rate and PHRR are larger. The addition of COPS adds aromatics to the polymer, which must cause an increase in smoke. It has been previously observed that PMMA nanocomposites show an increased time to ignition; this is unique behavior for nanocomposites. Perhaps the compatibility between the methacrylate-substituted clay and the methacrylate polymer are important in the cone calorimetric properties of the nanocomposite. This assertion is substantiated by the fact that the styrenic-substituted PS nanocomposite shows the best values.

Table 3. Cone calorimetric data for COPS-PMMA nanocomposites

Composition	Pure PMMA	2.5%COPS/PMMA	5%COPS/PMMA	15%COPS/PMMA	25%COPS/PMMA
t_{ign} (s)	31±1	32±3	34±1	39±2	45±1
PHRR (kW/m 2) (reduction)	779±22	737±10 (5)	689±9 (11)	629±14 (19)	663±30 (15)
t_{PHRR} (s)	94±14	99±8	94±4	78±1	59±1
Time to burn out (s)	256±1	269±2	280±2	304±4	305±10
Energy released through 150 s (MJ/m^2)	85±1	81±3	79±2	73±1	74±5
Average HRR (kw/m^2)	351±5	329±12	317±1	277±4	289±1
Total heat released (MJ/m^2)	90±1	88±4	88±1	84±1	88±1
Average mass loss rate (g/s m^2)	18.9±0.3	17.0±0.3	16.2±0.2	14.3±0.2	14.0±0.5
Mass loss at 150 s (%)	93±1	84±5	88±2	85±2	78±3

Average specific extinction area (m²/kg)	152±1	186±1	228±7	370±19	457±8

Table 4. Cone calorimetric data for MAPS modified clay PMMA nanocomposites

Composition	Pure PMMA	2.5%COPS/PMMA	5%COPS/PMMA	15%COPS/PMMA	25%COPS/PMMA
t_{ign} (s)	31±1	35±1	33±1	33±4	27±4
PHRR (kW/m 2) (reduction)	779±22	782±14 (0)	741±23 (5)	600±4 (23)	614±28 (21)
t_{PHRR} (s)	94±14	87±5	87±1	83±7	79±5
Time to burn out (s)	256±1	230±2	259±10	288±9	296±7
Energy released through 150 s (MJ/m²)	85±1	78±1	76±1	69±1	67±3
Average HRR (kw/m²)	351±5	344±1	320±8	280±48	263±50
Total heat released (MJ/m²)	90±1	79±1	83±2	80±12	78±14
Average mass loss rate (g/s m²)	18.9±0.3	17.4±0.5	15.8±0.4	14.3±0.3	12.9±0.5
Mass loss at 150 s (%)	93±1	94±3	87±2	83±2	84±2
Average specific extinction area (m²/kg)	152±1	168±16	196±2	234±4	243±1

The results for polypropylene nanocomposites are shown in Table 5, Table 6. The time to ignition, total heat released and the mass loss rates are constant for both systems. For MAPS the PHRR is only reduced at 25% clay and the largest increase in smoke is seen at this value while for COPS there is a significant reduction in PHRR even at 15% clay but this reduction is much larger at 25% clay and the smoke values parallel this change. The reduction in PHRR for PP-g-MA systems is on the order of 50% [2], significantly larger than the 35% observed in this work. There is no example of a virgin PP nanocomposite with which to compare but, since the presence of maleaic anhydride may lead to char formation, one may expect virgin PP to have a lower reduction.

Table 5. Cone calorimetric data for COPS-PP nanocomposites

Composition	Pure PP	2.5%COPS/PP	5%COPS/PP	15%COPS/PP	25%COPS/PP
t_{ign} (s)	43±7	47±2	45±1	37±1	38±2
PHRR (kW/m 2) (reduction)	1845±328	1953±163 (0)	1889±22 (0)	1448±74 (22)	1191±37 (35)
t_{PHRR} (s)	±8	84±2	79±5	80±14	62±9
Time to burn out (s)	229±7	212±6	197±1	208±3	222±5
Energy released through 150 s (MJ/m²)	115±7	113±3	109±1	107±3	101±12
Average HRR (kw/m²)	518±30	540±20	561±5	524±15	461±8

Total heat released (MJ/m^2)	118±6	114±4	111±1	108±3	102±19
Average mass loss rate (g/s m^2)	15±1	15.6±1.0	16.0±0.3	17.1±1.1	15.4±0.2
Mass loss at 150 s (%)	92±6	99±1	100±1	100±1	97±2
Average specific extinction area (m^2/kg)	530±76	470±14	490±14	631±37	831±5

Table 6. Cone calorimetric data for MAPS-PP nanocomposites

Composition	Pure PP	2.5%MAPS/PP	5%MAPS/PP	15%MAPS/PP	25%MAPS/PP
t_{ign} (s)	43±7	44±7	42±1	39±7	41±15
PHRR (kW/m 2) (reduction)	1845±328	2025±304 (0)	1738±240 (6)	1651±174 (11)	1139±12 (38)
t_{PHRR} (s)	97±8	102±3	103±11	105±8	101±14
Time to burn out (s)	229±7	223±12	230±8	214±4	238±6
Energy released through 150 s (MJ/m^2)	115±7	119±6	115±4	113±3	101±1
Average HRR (kw/m^2)	518±30	551±20	525±22	540±23	443±10
Total heat released (MJ/m^2)	118±6	123±4	120±5	115±3	105±3
Average mass loss rate (g/s m^2)	15±1	15.5±1.4	14.9±0.5	16.1±0.6	13.7±0.2
Mass loss at 150 s (%)	92±6	92±9	93±3	98±2	88±6
Average specific extinction area (m^2/kg)	530±76	620±45	652±28	628±28	709±7

The results for polyethylene are quite similar to those of polypropylene, (Table 7, Table 8). The mass loss rate and the total heat evolved are constant while the time to ignition decreases for both systems. There is a significant reduction in the PHRR at both 15 and 25% and the smoke increases at these levels also. Previous work has shown a reduction in PHRR in PE-clay nanocomposites in the range of 35% and these are comparable and do indicate that nanocomposite formation does occur [9].

Table 7. Cone calorimetric data for COPS-PE nanocomposites

Composition	Pure PE	2.5%COPS/PE	5%COPS/PE	15%COPS/PE	25%COPS/PE
t_{ign} (s)	74±6	73±3	73±1	66±3	59±8
PHRR (kW/m 2) (reduction)	2128±377	1869±35 (12)	2048±414 (4)	1643±37 (23)	1482±6 (30)
t_{PHRR} (s)	90±8	87±4	92±1	72±16	60±2
Time to burn out (s)	224±16	228±2	224±9	198±3	245±10
Energy released through 150 s (MJ/m^2)	108±7	116±2	115±5	111±1	97±17
Average HRR (kw/m^2)	503±20	516±10	529±19	569±4	414±2
Total heat released (MJ/m^2)	113±4	118±2	118±4	112±1	101±1
Average mass loss rate (g/s m^2)	15.2±1.0	15.5±0.5	16.4±0.9	18.0±0.5	13.1±0.2
Mass loss at 150 s (%)	94±6	96±2	100±1	100±1	95±1
Average specific extinction area (m^2/kg)	345±54	411±3	400±65	475±21	786±26

Table 8. Cone calorimetric data for MAPS-PE nanocomposites

Composition	Pure PE	2.5%MAPS/PE	5%MAPS/PE	15%MAPS/PE	25%MAPS/PE
t_{ign} (s)	74±6	68±6	63±2	56±5	45±1
PHRR (kW/m 2) (reduction)	2128±377	2088±199 (2)	1780±90 (16)	1678±322 (21)	1227±142 (42)
t_{PHRR} (s)	90±8	103±10	94±13	99±7	111±7
Time to burn out (s)	224±16	215±12	228±3	227±11	233±16
Energy released through 150 s (MJ/m^2)	108±7	110±3	106±3	100±4	97±3
Average HRR (kw/m^2)	503±20	523±6	481±12	456±13	428±5
Total heat released (MJ/m^2)	113±4	112±2	110±3	104±3	99±1
Average mass loss rate (g/s m^2)	15.2±1.0	16.6±0.3	14.5±0.2	14.7±1.3	14.8±1
Mass loss at 150 s (%)	94±6	100±1	93±2	94±5	95±4
Average specific extinction area (m^2/kg)	345±54	396±16	465±13	512±46	546±38

An observation that has previously been made by Gilman [2], [3] and in this laboratory is that a significant reduction in PHRR occurs when a nanocomposites is formed and an insignificant reduction occurs for immiscible systems. For instance, in this study a larger batch of COPS-modified clay was prepared and it was found that the PP nanocomposites that was formed from this material did not give a reduction in PHRR. TEM images confirmed that the material was a microcomposite and that nanocomposites formation never occurred, apparently due to scale-up problems with the reaction for the production of large amount of the COPS-modified clay. Since the cone calorimeter samples the bulk of the material, it may be a better indicator of nanocomposite formation than is TEM, which can only examine a small piece of the sample and then one must extrapolate to the bulk. The combination of XRD, TEM and cone calorimetry suggests that exfoliated nanocomposites are produced for COPS-PMMA and that intercalated or mixed immiscible-intercalated nanocomposites are produced for the other systems.

3.5. Evaluation of mechanical properties

The mechanical properties, including Young's modulus, tensile strength and elongation at break of all of the nanocomposites prepared in this study, together with the corresponding values of the virgin polymers have been evaluated and the data are presented in Table 9. For the most part, the presence of the clay does not have a large effect on the mechanical properties of the polymer. The kind of polymer modified clay is important; MAPS behaves better than COPS in maintaining or enhancing the tensile properties of these virgin polymers. Young's modulus was increased as the amount of the clay increases, except for COPS-PMMA. For tensile strength, MAPS nanocomposites show better data than COPS nanocomposites. All nanocomposites show a decrease in % elongation. For PMMA the tensile falls at high clay while the elongation is unchanged by the presence of clay. For PP the tensile falls at high clay while the elongation also shows a small decrease up to 15% modified clay for COPS and a great decrease for MAPS. The tensile for PE is constant across the range of clay while the elongation falls at high clay. There is some difference between COPS and MAPS, but it is not a large difference.

Table 9. Mechanical properties of COPS- and MAPS-polymer nanocomposites

Nanocomposite	Elongation (%)	Modulus (GPa)	Tensile strength (Mpa)

Mechanical properties of poly(methyl methacrylate) nanocomposites			
PMMA	1.9±0.7	1.830±0.507	28.93±5.65
2.5%Cops/PMMA	2.0±0.6	2.003±0.321	29.58±13.15
5%Cops/PMMA	2.0±0.7	1.810±0.496	17.90±2.18
15%Cops/PMMA	1.1±0.5	1.554±0.080	5.68±3.17
25%Cops/PMMA	1.0±0.3	1.602±0	6.64±0
2.5%Maps/PMMA	2.5±1.0	1.905±0.282	47.10±16.14
5%Maps/PMMA	1.7±0.5	1.844±0.177	30.21±11.65
15%Maps/PMMA	1.4±0.4	2.446±0	9.40±5.30
25%Maps/PMMA	1.0±0.2	1.361±0.239	7.70±0.21
Mechanical properties of polyethylene nanocomposites			
PE	96.0±17.2	0.094±0.004	10.41±0.59
2.5%Cops/PE	80.9±17.8	0.095±0.006	9.64±0.59
5%Cops/PE	82.9±14.4	0.098±0.010	10.35±0.94
15%Cops/PE	72.7±10.0	0.125±0.005	8.87±0.64
25%Cops/PE	57.1±10.1	0.218±0.028	8.49±0.36
2.5%Maps/PE	89.8±4.2	0.089±0.007	10.16±0.69
5%Maps/PE	76.4±17.6	0.099±0.003	10.13±0.54
15%Maps/PE	73.7±5.9	0.119±0.016	7.91±0.83
25%Maps/PE	61.0±4.4	0.122±0.007	8.16±0.37
Mechanical properties of polypropylene nanocomposites			
PP	708±20	1.229±0.122	32.0±2.0
2.5%Cops/PP	338±176	1.381±0.102	31.34±0.80
5%Cops/PP	362±141	1.570±0.470	30.80±2.20
15%Cops/PP	363±95	2.154±0.621	25.20±1.70
25%Cops/PP	55±18	2.369±0.440	23.61±1.42
2.5%Maps/PP	403±120	1.428±0.437	29.60±0.60
5%Maps/PP	72±64	1.523±0.258	29.10±1.05
15%Maps/PP	32±7	1.831±0.185	27.90±3.30
25%Maps/PP	20±4	2.203±0.390	24.0±2.10

4. Conclusions

Both of these polymeric clays offer an advantage in thermal stability when compared to conventional ammonium salts; this is especially true for the COPS clay. When a clay that is quite compatible with polypropylene is used, maleation is not required and one can make polypropylene nanocomposites by the direct blending of the polymer and the clay. It is quite possible that one can prepare an exfoliated polypropylene nanocomposite by melt blending at higher shear. The degradation begins at higher temperatures for these systems and this may enable melt processing of polymers which require higher temperature. It is clear that XRD and TEM alone are not enough to characterize the type of nanocomposite that has been produced and that cone calorimetry offers an advantage, since it samples the bulk material rather than only a small piece.

Acknowledgements

References

[1] Su S, Jiang DD, Wilkie CA. Accompanying paper.

[2] J.W Gilman, T Kashiwagi, M Nyden, J.E.T Brown, C.L Jackson, S Lomakin, *et al.* S Al-Malaika, A Golovoy, C.A Wilkie (Eds.), *Chemistry and technology of polymer additives*, Blackwell Scientific (1999), pp. 249-265

[3] Gilman JW, Kashiwagi T, Giannelis EP, Manias E, Lomakin S, Lichtenham JD, Jones P. In: Le Bras M, Camino G, Bourbigot S, Delobel R, editors. *Fire retardancy of polymeric materials, the use of intumescence*, Royal Society of Chemistry, Cambridge, p. 203–21.

[4] Kurata M, Tsunashima Y. In: Brandrup J, Immergut EH, Grulke EA, editors. 1999, p. VII/1–84.

[5] D Wang, J Zhu, Q Yao, C.A Wilkie. *Chem. Mater*., 14 (2002), pp. 3837-3843

[6] M Zanetti, G Camino, D Canavese, A.B Morgan, F.J Lamelas, C.A Wilkie. *Chem. Mater*., 14 (2002), pp. 189-193

[7] Balabanovich AI, Schnabel W, Levchik GF, Levchik SV, Wilkie CA. In: Le Bras M, Camino G, Bourbigot S, Delobel R, editors. *Fire retardancy of polymeric materials, the use of intumescence*, Royal Society of Chemistry, Cambridge, p. 236–251.

[8] J Zhu, P Start, K.A Mauritz, C.A Wilkie. *Polym. Degrad. Stab*., 77 (2002), pp. 253-258

[9] J Zhang, C.A Wilkie. *Polym. Degrad. Stab*., 80 (2003), pp. 163-169

[10] C.F Cullis, M.M Hirschler **The combustion of organic polymers.** Clarendon Press, Oxford (1981)